

**Soil Moisture Retrieval Using the Passive/ Active
L- and S- Band Radar/Radiometer**

J. Bolten¹, V. Lakshmi¹, and E. Njoku²

¹Dept. of Geological Sciences

University of South Carolina, Columbia, SC 29208

jbolten@geol.sc.edu

vlakshmi@geol.sc.edu (**corresponding author**)

²Jet Propulsion Laboratory

California Institute of Technology, Pasadena, CA 91109

eni.g.njoku@jpl.nasa.gov

Abstract

In the present study, remote sensing of soil moisture is carried out using the Passive and Active L- and S-band airborne sensor (PALS). The data in this paper were taken from 5 days of overflights near Chickasha, Oklahoma during the 1999 Southern Great Plains (SGP) experiment. Presently, we analyze the collected data to understand the relationships between the observed signals (radiometer brightness temperature and radar backscatter) and surface parameters (surface soil moisture, temperature, vegetation water content, and roughness). In addition, a radiative transfer model and two radar backscatter models are used to simulate the PALS observations. An integration of observations, regression retrievals and forward modeling is used to derive the best estimates of soil moisture under varying surface conditions.

1.0. Introduction

The principal variables in land-surface hydrology are soil moisture, surface temperature, vegetation, precipitation and streamflow. Of these, surface temperature, vegetation and precipitation are currently observed using satellites, and streamflow is routinely observed at in-situ watershed locations. Soil moisture remains the only variable not observed (or observed very sparsely) either in-situ or via remote sensing.

Numerous studies have shown the influence of soil moisture on the feedbacks between land-surface and climate, which in turn affect the dynamics of the atmospheric boundary layer and have a direct relationship to weather and global climate [1]-[4]. Chang et al. [5] have shown the influence of spatial variations of soil moisture and vegetation on the development and intensity of severe storms, whereas [6] demonstrated the ability of soil moisture to influence surface moisture gradients and to partition incoming radiative energy into sensible and latent heat. Better understanding of the processes involved in the forcing of, and responses to, Earth's changing environment is needed in order to accurately assess, predict and evaluate the relationship between the global hydrologic cycle, weather and climate change. For this to be accomplished, it is necessary to intimately understand the relationship of soil moisture to these phenomena on small and large-spatial scales. Unfortunately, complicating these overall goals is our inability to completely observe large-scale hydrologic land-surface interactions. Remote sensing enables us to estimate large-scale soil moisture for the purpose of modeling the two-way interaction between land and atmosphere, making it possible to understand the nature of

global climate. This paper examines multiple techniques used to retrieve land-surface parameters using microwave remote sensing. Given the near linear relationship between soil moisture and microwave emission, many prior studies [7-10] have focused on regressions between remotely sensed observations and observed surface soil moisture or comparisons between aircraft/satellite retrievals and in-situ observations. Another common method of soil moisture estimation analysis involves modeling the microwave emission of vegetated and bare soil surfaces based on the physical parameters of the media [11-13]. In this paper we attempt to combine these methods using observations from PALS, statistical regressions (between retrievals and observations of soil moisture), and physically based forward modeling of the sensor for the purpose of near surface (0-5cm) soil moisture retrieval. In order to investigate these relationships, the data were stratified into three vegetation water content regimes: low ($<0.25 \text{ kg m}^{-2}$), medium ($0.25\text{-}3.0 \text{ kg m}^{-2}$), high ($>3.0 \text{ kg m}^{-2}$), observed during the Southern Great Plains 1999 (SGP99) experiment. The fairly wide range of land-surface conditions encountered in SGP99 permits study of the advantages and drawbacks of passive and active remote sensing under varying vegetation, soil moisture and roughness conditions.

Previous investigations have shown that passive microwave remote sensing is effective in the study of soil moisture [14-20] and precipitation [21-24]. These efforts have qualitatively demonstrated the theoretical sensitivity of microwave brightness temperature to soil moisture variations in varying media [25]-[26]. Overlying vegetation and atmospheric moisture have been shown to have less effect on soil emission at longer microwave wavelengths [27]. In addition, lower frequencies within the 1-6 GHz range

have an increased soil sensing depth and provide a large contrast between wet and dry soil. This frequency range has therefore in effect become the main focus of remote sensing of soil moisture. Aside from previous SGP campaigns [28], the majority of research done using low frequency microwave radiometry has been focused on smaller catchments over uniform ground conditions [29]-[30]. There is still a need for validating and comparing models and algorithms in large-scale field experiments.

2.0. Background

Microwave radars observing the land-surface measure the backscattering coefficient, a dimensionless quantity representing the scattering from the soil and vegetation components of the surface. Scattering from the soil depends on both the dielectric constant (which is affected by soil moisture) and the surface roughness. An increase in soil moisture results in an increase in surface backscatter, giving a positive relationship whose slope depends on the roughness and vegetation characteristics. The transmit-receive polarization combination associated with the backscattering coefficient is denoted by σ_{ij}° , where $i,j = H$ or V (horizontal or vertical polarizations). Backscatter is expressed as decibels (dB). Depending on roughness and provided bare to low vegetation cover, these values can change roughly between -5 and -10 dB for both VV- and HH-polarizations over the dynamic moisture range from dry to saturation.

As the moisture content in a soil increases, so does its surface reflectivity, r . This results in a decrease in the emissivity, $1-r$, of the soil. The resulting emissivity changes from the surface are used in the interpretation of data from microwave radiometers measuring the

emission from the surface. The emissivity has a strong influence on the radiated brightness temperature of the surface in the microwave region. The brightness temperature, T_B , is proportional to the product of the physical temperature and the emissivity of the surface [18, 31]. Brightness temperature has been shown to have a linear relationship with surface soil moisture [32]. Because of the large difference in emissivity of dry and wet soil, a comparison of the relative brightness temperatures of the soils can be used to detect soil moisture [27].

In the present study, data from the PALS instrument were used to retrieve soil moisture in the Southern Great Plains Little Washita, Oklahoma region. PALS was developed to study the utilization of dual-frequency, dual-polarization, passive and active measurements for remote sensing of ocean salinity and soil moisture. The instrument operates at 1.4 and 2.69 GHz in the radiometer channels and 1.26 and 3.15 GHz in the radar channels. PALS utilizes a multi-frequency, multi-polarized design, and is capable of acquiring simultaneous radar and radiometric signatures of land and ocean surfaces. The radiometer receives coincidental vertical and horizontal emission and the radar transmits vertical or horizontal polarization and receives these two linearly polarized radar echoes simultaneously. A more thorough description of the PALS specifications and applications can be found in [33]. An analysis of PALS soil moisture observations during SGP99 has been performed; the approach and results are detailed by Njoku et al. [34]. Data collected during the study were calibrated and geometrically corrected for aircraft navigational and attitude variations and organized for each flight line overpass of the individual agricultural fields. The instrument provided simultaneous collection of

horizontally and vertically polarized L- and S- band brightness temperature and backscatter coefficients, nadir-looking thermal infrared surface temperature, footprint latitude and longitude position and aircraft altitude. The unique active/passive design provides valuable information on the corresponding effects of varying vegetation, surface types and soil moisture on the radar and radiometer responses.

PALS was flown during the Southern Great Plains Field Experiment, July 8th to 20th, 1999, on a C-130 aircraft. The experiment included a variety of airborne C-, S-, and L-band microwave instruments to provide large-scale soil moisture mapping in the Little Washita Basin (603 km²), near Chickasha, Oklahoma. The present study discusses the PALS instrument exclusively; a description of additional instruments used during SGP99 and experiment details can be found on the experiment web site (http://daac.gsfc.nasa.gov/CAMPAIGN_DOCS/SGP99/index.shtml). PALS flew over the Little Washita Watershed at a nominal altitude of 3,000 feet with an approximate footprint size of 300 x 400 m for a total of 6 days. Flight lines were selected over a range of field sites to provide a comprehensive analysis of varying ground cover. The land conditions and time of study of the Little Washita Basin are ideal for evaluating new sensor systems and algorithms. Forest cover within the watershed is very sparse and typically follows streams constituting a small portion of the watershed [34]. The basin consists mostly of rolling hills (maximum relief is less than 200m), rangeland and pasture. For purposes of this paper, the representative texture for the surface layer soil is taken to be 30% sand and 20% clay. Within the watershed, the ground truth data collection included eleven field sites (0.8 Km x 0.8 Km), chosen in five types of land-cover: rangeland, wheat, corn,

alfalfa and fallow, ranging in vegetation water content from 0-7.18 kg/m² (Table I). Collected ground data applicable to this paper include: gravimetric soil moisture (0 – 2.5 and 0 - 5 cm), surface roughness, soil bulk density, and vegetation water content as described in [34]. It should be noted that in this study, the 0 – 5 cm gravimetric soil moisture is used exclusively (instead of volumetric soil moisture) due to possible bulk density in-situ measurement error. When applied in the following analysis, a bulk density value of 1.28 g cm⁻³ has been used.

Weather conditions were ideal during the study, including a major rain event on the third day (July 10th, 1999). This allowed a subsequent drydown period to be observed throughout the basin (a change in gravimetric soil moisture content from about 24.3% to 3.4% over a period of 8 days). The precipitation was non-uniform throughout the basin (varying from 31.0 mm in the western part of the watershed to approximately 9.6 mm in the eastern regions), causing a heterogeneous soil moisture pattern across the watershed [36]. Although the weather and vegetation conditions presented a sufficient range of soil moisture and vegetation water content, the heterogeneous nature of the moisture patterns within the watershed do not allow for the analysis of areas with both high vegetation and moisture. This presents problems in the following regression analysis and must be considered upon interpretation of the results.

3.0. Soil Moisture Estimation Techniques

Three techniques are examined in this paper for retrieving soil moisture from the PALS microwave emission and backscatter observations of the soil-canopy system; (a) Regression analysis, (b) Passive physical model and (c) Active physical model. In this initial study an attempt has not been made to create a combined passive/active algorithm, rather the analyses (for radiometer and radar) have been carried out separately.

In applying physical models it is important to choose soil surface and vegetation parameters with as much realism as possible while ensuring representative characterization of the field sites, and it is desirable that the parameterizations used be consistent between the passive and active models. The models in this study assume a soil type (sandy loam) representative of the SGP region, with sand and clay fractions of 30% and 20%, respectively. Dielectric constant values were determined using the equations of Dobson et al., 1985. This dielectric model uses sand and clay mass fractions along with bulk density (average of in-situ) to describe soil texture. The PALS incidence angle of $\theta = 39^\circ$ was used in the model calculations. We have focused the modeling results on the low vegetated fields due to the fact that the radar models simulate these conditions best.

4.0. Regression Analysis

It has been shown that radiometric and radar soil-moisture sensitivities to soil moisture vary differently depending on vegetation characteristics, frequency and polarization. By analyzing multiple channels over a varied vegetation range we expect to improve our soil moisture prediction potential. This was investigated by comparing results of multiple

regressions performed on the collocated radiometer/scatterometer measurements and in-situ gravimetric soil moisture measurements.

For the multiple linear regression analyses an equation of the form

$$m_j^* = a_0 + \sum_{i=1}^N a_i d_{i,j} \quad (1)$$

was used, where $d_{i,j}$ are the radiometer or radar data (brightness temperatures or backscattering coefficients) in channel i and data point j , corresponding to a collocated field site. N is the number of channels included in the regression, a_0 and a_i are the derived regression coefficients, and m_j^* are the regression fit estimates of soil moisture.

Assuming a uniform temperature in the top 0–5 cm soil layer, the microwave brightness temperature T_B (θ_i) can be expressed as

$$T_{\text{bq}}(\theta_i) = e_q(\theta_i)T_s \quad (2)$$

where θ_i is the incidence or view angle of the sensor, $q = \{v, h\}$ refers to the horizontal and vertical polarizations of the emitted radiation and T_s is the surface temperature. Here, for a given T_s , the emissivity, $e_q(\theta_i)$, of the surface is proportional to the brightness temperature. Given the near-linearity of the m_g versus T_B relationship, we are able to effectively evaluate interactions between soil and vegetation parameters and the retrieved brightness temperatures using multiple linear regressions. Radar backscatter has been shown to have a less linear relationship to soil moisture than radiometric brightness temperature [31]-[39]. Nevertheless, the backscatter coefficients are included in the regression analysis to further examine these findings and also to determine to what extent multiple channels, both active and passive, may improve soil moisture retrieval.

A series of regression models were generated using a best subset regression technique. The models use the maximum coefficient of multiple determination, R^2 , criterion by first examining all one-band regression models and selecting the model giving the largest R^2 value. Based on the R^2 , a group of best subsets is then selected for further regression analysis. The benefits of using multiple channels can be investigated by comparing the predictive capabilities of the sensors using 1, 2, 3, and 4 channels.

Tables IIa and IIb list the results of the best subset regression analyses applied to all vegetation types. It is observed for the passive case that combining multiple channels provides only a slight increase in soil moisture accuracy (an increase in R^2 of 0.02). This is a result of the high correlation provided by use of the single LH channel. However combining multiple active channels gives a significant increase in the proportion of explained variation (an increase in R^2 of 0.36), a consequence of the radar having a greater sensitivity towards roughness and vegetation characteristics. The inclusion of multiple channels helps in characterization of the scattering due to roughness and vegetation, and hence increases the soil moisture estimation accuracy.

Using the five days of available collocated data, two (or three) days were regressed and predictions were performed on the remaining three (or two) days of data. Figure 1 shows the regression results over all the fields using the four passive channels noted in Table IVa. The plot shows the predicted and in-situ soil moisture values for July 12th, 13th, and 14th, (based on the regression fit derived using data for July 9th and July 11th). The

regression estimate has an R^2 value of 0.96, with predictions accurate within 1.83 % of observed gravimetric soil moisture. Table III shows the passive regression results for all vegetation types using different days as the control group. The regression estimates have standard error of m_g less than 2.0% for most cases.

The same approach was applied using the active PALS channels. Figure 2 shows the results for the radar channel regressions using the same regression/prediction scheme as in Figure 1. The four channel combination (LHH, LVV, SVV and SHHV) results in a standard error of 2.63% gravimetric soil moisture and an R^2 value of 0.67. A summary of the remaining regression/prediction models is found in Table III. As expected from the best subset analysis, the active channels did not perform as well as the radiometer channels but demonstrate the radar capability to retrieve soil moisture with reasonable accuracy over the varied vegetation conditions encountered in the SGP region.

Caution must be used when interpreting the regression results; the limited number of flight lines and sampled field sites allow for only 36 co-located (within 300m of aircraft footprint) data points to be used in the study. The correlation of the predicted points weigh heavily on those used for the initial regression. An ideal data set should include the full range of soil moisture and vegetation conditions encountered during the study, enabling regressions and predictions to be performed for the full spectrum of possible environments. Unfortunately, this data set did not span a full range since there were no fields with simultaneous high soil moisture and high vegetation water content.

Deviations between the predicted and observed moisture can also be attributed to sampling and measurement error during SGP99. One source of sampling error is the collocation error (location uncertainty of the PALS footprint positions and field data collection sites). With large distances (300 m used to assign collocation), the PALS footprints may view different field conditions from the assumed conditions of each field. In addition, the collection of gravimetric soil moisture is not exact and will also introduce error into the estimates. The time of the PALS flights over the individual field sites and the field data collection in those sites must also be considered, as differences in time will cause PALS and in situ soil moisture and temperature values to be different.

5.0. Forward Model for Passive Radiation Transfer

A physically based microwave emission model was used to further investigate the relative sensitivities of L- and S- band passive measurements to surface soil moisture. The approach was based on a model of microwave emission from a layered soil-vegetation-atmosphere medium for frequencies in the range 1-20 GHz [13]. The radiative transfer model assumes that the vegetation canopy consists of a uniform layer above the soil (introduced in the model by optical thickness, τ_c , vegetation water content, w_c , and single scattering albedo, ω). The optical thickness parameter is dependent on w_c and has been shown to follow an approximately linear relationship, as described in [13]:

$$\tau_c = bw_c / \cos \theta \quad (3)$$

where the $\cos \theta$ factor accounts for the slant observation path through vegetation and the b parameter is a coefficient that depends weakly on vegetation type and is approximately

proportional to frequency [40]. A summary of model inputs is shown in Table IV. All parameters were fixed in the model with the exception of those collected during the SGP99 study: gravimetric soil moisture, vegetation water content and surface temperature. A constant surface roughness value $h=0.2$ was been assumed for the fields, based on observed roughness data values. Also an average bulk density value of 1.28 g cm^{-3} was used for all fields. The polarization mixing parameter Q was assigned a value of 0.2 for all simulations. Wigneron et al., [41] have shown this value to be valid for similar land-cover conditions at 1.4 GHz. An opacity coefficient value of 0.1 and 0.19 was assumed for all vegetated surfaces at L and S- band, respectively. Jackson and Schmugge [41] have estimated these values from experimental data at 1.41 GHz by parameterization of the transmissivity of the vegetation layer based on vegetation water content.

Surface parameters collected during the study were input into the model collocated by field type and day of study. All the variables were collected daily except for vegetation water content, bulk density and surface roughness, whose values were assumed to remain constant for the duration of the study. The model assumes homogeneous surface conditions giving averaged effective values over the radiometer footprint. The soil dielectric constant was computed for given bulk density, frequency, gravimetric moisture content, sand and clay fractions, and temperature using empirical relations taken from [42].

Figure 3 shows a comparison between the average estimated brightness temperature ($\overline{T_B} = (T_{BLH} + T_{BLV})/2$) and the PALS observations over all fields during SGP99. The $\overline{T_B}$

calculation has been shown by [43] to summarize the effects of both vertical and horizontal polarization and is used here for simplification. The scatterplot indicates that the radiative transfer model agrees well with the PALS observations, giving a standard error between estimated and measured brightness temperature ($\overline{T_B}$), of less than 12 K. This agreement is representative of estimated brightness temperatures for SH- and SV-bands. The model underestimates the PALS brightness temperature collected over all three vegetation types, with best agreement ($R^2 = 0.9$) in the low vegetated fields. This is due to the fact that the model underestimates the effects of the vegetation cover. Calculations show that these discrepancies can be reduced if the parameters Q , b are also allowed to vary. These results are not presented here.

A combination forward model-statistical regression-inverse model technique was used to retrieve soil moisture over all the fields. Using this method, two (or three) days of surface parameter data were input to the model and the resulting brightness temperatures were regressed against the corresponding PALS brightness temperatures (to calibrate or train the model to the observations). The resulting regression coefficients could then be applied to the remaining three (or two) days of surface parameter observations to derive a set of modeled brightness temperatures consistent with the PALS data. The rationale is that although linear regression alone is capable of providing reasonably accurate moisture estimates, a more robust approach should be obtainable by combining regression estimates with forward models. Using this method we can ‘train’ the model for the region by regressing a portion of the forward model outputs with observations from PALS and apply through model inversion the resulting coefficients to the remaining PALS data.

An iterative least-squares minimization algorithm was applied to the modeled and computed brightness temperatures, with soil moisture adjusted (spanning the dynamic range: $m_g = 3$ to 35%) until the difference between the modeled and computed brightness temperatures, (H- and V- pol) was minimized. Results of the predicted low vegetation, L-band model are shown in Figure 4. The model gives a relatively good prediction of soil moisture for July 12th, 13th and 14th over the low vegetated fields (standard error = 2.23% m_g).

Multiple models were run using different combinations of days for the regression scheme for both the L and S-band radiometer wavelengths. The soil moisture retrieval estimates from the models over all vegetation ranges are summarized in TableV. Both the L- and S-band outputs of the models give relatively consistent results, however, there is one instance (using July 11th, 12th and 14th for the regression in the L-band model) that gives an extraordinarily low standard error of 0.6% m_g . This is a result of the low number of prediction values available, 3, which happen to be very close to the observed moisture values and is not considered representative of the entire dataset. The models have shown that both the 1.4 and 2.7 GHz channels of the radiometer are successful in predicting soil moisture through low vegetation conditions. The soil moisture predictions obtained at S-band are reasonably close to those obtained from the L-band analysis, however they result in slightly higher standard error (0.48% m_g on average). The brightness temperature dependence on the 0- to 5-cm gravimetric soil moisture is found to be stronger for the 1.4 GHz channel as confirmed in the regression analysis.

6.0. Forward Models for Active Backscatter

Prior investigations utilizing microwave scatterometers for retrieval of surface variables have shown the benefits of long wavelength, co-polarized backscatter measurements when applied to surface roughness and land-cover separability [44]-[46]. These studies have demonstrated the strong degree to which σ^0 is a function of surface roughness, vegetation and near surface soil moisture. The active channels were also examined for soil moisture sensitivity.

We utilize here two simplified scattering models developed by Dobson et al. [20], and Dubois et al [37]. Whereas the Dobson scattering model was developed from truck-mounted scatterometer data (LHH) over varying vegetation types, the Dubois empirical model was derived to describe truck-mounted copolarized backscatter measurements (LVV, LHH) of bare surfaces as a function of surface roughness, dielectric constant, incidence angle and frequency. The range of surface conditions encountered during SGP99 is close to that used to train both the above models and are assumed applicable when applied to the PALS frequency at L-band (for the Dobson model) and L- and S-band (for the Dubois model).

The Dobson scattering model uses the small perturbation approach to compute total LHH backscatter as a sum of surface scatter from the soil, σ_{surf}^0 , volume scatter from the canopy, σ_{vol}^0 , and scatter from surface/volume interaction, σ_{int}^0 .

$$\sigma_{tot}^0 = \sigma_{surf}^0 + \sigma_{vol}^0 + \sigma_{int}^0 \quad (4)$$

The model computes σ_{vol}^0 and σ_{int}^0 using empirically derived expressions as described in [20], involving wavelength, RMS roughness, surface correlation length, dielectric constant, and canopy albedo. A summary of the model parameters required is shown in table VI. Since the Dobson model is based on a more detailed parameterization than the Dubois model, it is more susceptible to error in comparing modeled backscatter with PALS observations if these parameters are not accurately known.

The Dubois model was developed using a variety of sources of training data: incidence angle, dielectric constant, RMS height, and wavelength to empirically derive equations for the HH- and VV- polarized backscattering cross-sections σ_{hh}^0 and σ_{vv}^0 for varying soil moisture and surface roughness within the 1.5 GHz – 11 GHz range. The vegetation effects are excluded in this version of the Dubois model, optimizing it for bare surfaces and is used here as a comparative tool for the SGP99 low vegetated fields. The model computes the copolarized backscattering cross-sections σ_{hh}^0 and σ_{vv}^0 as functions of incidence angle, θ , real part of the dielectric constant, ϵ' , and RMS height of the surface, s , [37]. Caution must be used when applying empirical models to datasets other than those used for their development. In our case the model was determined to be sufficient based on the range of surfaces that it was developed for and the scatterometer data that it has been applied to: AIRSAR, SIR-C, POLARSCAT, and RASAM.

Figure 5 shows a comparison of the Dobson model and PALS backscatter (LHH) over the low vegetated fields. The scattering model was developed for calculating surface scatter at 1.28 GHz, and therefore a comparison with the PALS 3.15 GHz frequency cannot be performed. The model displays a similar variation of backscatter with gravimetric soil moisture to that observed with PALS. Within the observed ranges of surface and canopy cover conditions the active model bounds the majority of observed data but shows more variance than the passive model. These deviations can be attributed to heterogeneity effects and model parameterization errors. The parameter values used in Table VI, to which the radar is more sensitive than the radiometer, can at best be considered first order approximations to the actual variability across the SGP region.

Figure 6 shows the soil moisture estimation for July 9th, 12th and 14th over bare and low vegetated (biomass < 0.25 kg m⁻²) fields using the Dobson model. The model-based estimates underpredict all but one of the observed moisture values. Surprisingly, better model-based estimates are obtained for the high-vegetated fields (not shown). This could be a result of the model having been developed with more applicability to corn canopies, as encountered in the high-vegetated fields rather than to pasture and bare conditions as encountered in the low vegetated fields.

Figure 7 presents both the σ_{hh}^0 and σ_{vv}^0 responses of the Dubois model compared to the measurements from the PALS data collected over the low vegetated fields. This model has a better correlation ($R^2=0.6$) with the PALS backscatter compared with the Dobson model, (over low vegetated fields). It should be noted that the low-vegetated fields

include bare fields and low vegetated fields ($<0.25 \text{ kg/m}^2$), but still give a good response when applied to the bare-surface empirical model.

The forward-regression-inverse technique was applied to the Dubois model using the LHH channel for comparison to the Dobson model. A series of regressions and predictions were performed for a combination of the five days of collocated SGP99 data. The observed in-situ versus predicted gravimetric soil moisture for July 12th and 14th over the low vegetated fields is shown in Figure 8. The error in predicting soil moisture over these low vegetated fields giving a standard deviation of 2.79% m_g and an R^2 value of 0.64 represents the cumulative error of the algorithm (in-situ data, regressions, inversions).

Both active models provide reasonable estimates of soil moisture under similar conditions. The comparison with in-situ data shows that the Dobson model underestimates moisture more than the Dubois model for the SGP99 field conditions. However, this underestimation is not a result of our model calibration. As stated earlier, deviations of estimated from in-situ soil moisture values for the Dobson model are possibly a result of differences between the parameterizations used to derive the original model and values assumed for the SGP99 experiment. It is also noted that given the relationship between the dielectric constant of soil and backscatter coefficient, as well as the correlation with surface roughness and vegetation, the presence of vegetation could result in overestimated surface roughness and/or underestimated soil moisture. A

summary of the L-band performance of both active models is provided in Table VII for the low vegetated fields.

8.0. Conclusions and Discussion

A combination of multiple regression analyses and contrasting evaluations with microwave physical models have been used in this study for evaluation of the L-band passive and active sensitivity to near surface soil moisture. A distinct soil moisture signal was observed for the highly vegetated fields as well as for the bare and low-vegetated fields. In studying the capabilities of PALS, the results have:

- 1) Illustrated the sensitivity of remote sensing measurements (active and passive) to soil moisture in the presence of variable vegetation cover and heterogeneity.
- 2) Improved our knowledge of the emission (passive) and scattering (active) characteristics of microwave interactions with soils at different frequencies and polarizations, and the effects of ancillary variables such as vegetation water content, surface roughness and temperature.

The prediction techniques investigated exhibited varying soil moisture retrieval potential. Most of the estimates using passive channels provided between 2% and 3% accuracy in comparisons with the in-situ gravimetric soil moisture. Estimates using the active channels provided accuracies mostly in the 2-5% range. Part of the error in these estimates is contributed by in situ sampling error and collocation error.

This paper has provided a framework for studying active and passive observations of the land-surface under diverse conditions. Statistically based regressions were developed

although these are of limited scope considering the small size of the observational SGP99 data set. The estimation of soil moisture based on physical forward models was motivated by a desire to apply understanding of the radiative transfer and backscatter processes to more generally applicable retrieval methods. It has been shown that physically based methods coupled with regression analyses can serve as useful tools for this and other studies.

The physically based emission model is found to correlate well with the PALS data collected over bare and low vegetated (biomass $< 0.25 \text{ kg m}^{-2}$), medium ($0.25\text{-}3.0 \text{ kg m}^{-2}$), and high ($>3.0 \text{ kg m}^{-2}$) vegetated fields, with LH-band brightness temperature standard error of 6.6K, 9.9K, and 6.17K respectively. The backscatter models were found to provide additional information, but with more variance due to vegetation and heterogeneity effects. We have not attempted in this study to merge the active and passive components into a single retrieval technique. A combined active/passive technique could serve as a method to retrieve multiple surface variables: viz., soil moisture, surface temperature, surface roughness, and vegetation water content. Given the rather limited scope of the SGP99 in situ sampling and range of vegetation and soil moisture conditions observed, additional more detailed study (currently in progress) will be needed to develop such a combined approach. Future field experiments to acquire a larger quantity of collocated field data covering a wider dynamic range of environmental conditions will facilitate these efforts.

References

1. J. Shukla and Y. Mintz, "Influence of land-surface evapotranspiration on the Earth's climate," *Science*, vol. 215, pp. 1498-1500, 1982.
2. T. Delworth and S. Manabe, "The influence of soil wetness on near-surface atmospheric variability," *Journal of Climate*, vol. 2, pp. 1447-1462, 1989.
3. K.L. Brubaker and D. Entekhabi, "Analysis of feedback mechanisms in land-atmosphere interaction," *Water Resources Research*, vol. 32, pp. 1343-1357, 1996.
4. R.A. Pielke Sr. "Influence of the spatial distribution of vegetation and soils on the prediction of cumulus convective rainfall," *Reviews of Geophysics*, vol. 39-2, 2001.
5. J. T. Chang and P. J. Wetzel, "Effects of spatial variations of soil moisture and vegetation on the evolution of a prestorm environment: A numerical case study," *Monthly Weather Review*, vol. 119, 1991.
6. T.E. Engman, "Soil moisture, the hydrologic interface between surface and ground waters." *Remote sensing and geographic information systems for design and operation of water resources systems (Proceedings of Rabat symposium S3, April 1997)*. International Association of Hydrological Sciences, vol. 242, 1997.
7. J. Li and S. Islam. "On the estimation of soil moisture profile and surface fluxes partitioning from sequential assimilation of surface layer soil moisture." *Journal of Hydrology*, vol. 220, pp. 86-103, 1999.
8. T.J. Schmugge, J. R. Wang, and G. Asrar, "Results from the pushbroom microwave radiometer flights over the Konza prairie in 1985." *IEEE Transactions on Geoscience and Remote Sensing*, vol. 26. 590-596, 1988.
9. J.R. Wang, J.C. Shuie, T.J. Schmugge, and E.T. Engman, "Mapping soil moisture with L-band radiometric measurements." *Remote Sensing of the Environment*, vol. 27, 305-312, 1989.
10. J.R. Wang, J.C. Shuie, T.J. Schmugge, and E.T. Engman. "The L-band PBMR measurements of surface soil moisture in FIFE." *IEEE Transactions in Geoscience and Remote Sensing*, vol. 28, 906-914, 1990.
11. M. Owe, A. A. Van de Griend, and A. T. C. Chang, "Surface moisture and satellite microwave observations in semiarid southern Africa," *Water Resources Research*, vol. 28, pp.829-839, 1992.
12. J. P. Wigneron, Y.H. Kerr, A. Chanzy, and Y. Q. Jin, "Inversion of surface parameters from passive microwave measurements over a soybean field," *remote Sensing of the Environment*, vol. 46, pp.61-72, 1993.
13. E.G. Njoku, L. Li. "Retrieval of land surface parameters using passive microwave measurements at 6-18 GHz." *IEEE Transactions on Geoscience and Remote Sensing*, vol. 37, pp.79-93, 1999.
14. M. Owe, A.A. Van de Griend, R. de Jeu, J.J. de Vries, E. Seyhan, and E.T. Engman. "Estimating soil moisture from satellite microwave observations: Past and ongoing projects, and relevance to GCIP." *Journal of Geophysical Research-Atmospheres*, vol. 104, pp. 19735-19742. 1999.
15. T.J. Jackson and T.J. Schmugge. "Passive microwave remote sensing system for soil moisture, some supporting research." *IEEE Transactions on Geoscience and Remote Sensing*. vol. GE-27, pp. 225-235. 1989.

16. T.J. Jackson, "Measuring surface soil moisture using passive microwave remote sensing." *Hydrological Processes*, vol. 7. pp. 139-152. 1993.
17. J.K. Hollenbeck, T.J. Schmugge, M.G. Hornberger, J.R. Wang. "Identifying soil hydraulic heterogeneity by detection of relative change in passive microwave remote sensing observations." *Water Resources Research*, vol. 32-1, pp. 139-148, 1996.
18. L.P. Simmonds and E.J. Burke. "Estimating near-surface soil water content from passive microwave remote sensing-an application of MICRO-SWEAT." *Hydrological Sciences-Journal-des Sciences Hydrologiques*, vol. 43-4, pp. 521-534. 1998.
19. T.J. Jackson, "Multiple resolution analysis of L-band brightness temperature for soil moisture". *IEEE Transactions on Geoscience and Remote Sensing*, vol. 39, no. 1. pp. 151-164, 2001.
20. M.C. Dobson, F.T. Ulaby. "Preliminary evaluation of the SIR-B response to soil moisture, surface roughness, and crop canopy cover." *IEEE Transactions on Geoscience and Remote Sensing*, vol. GE-24, 1986.
21. W.S. Olson, P. Bauer, N.F. Viltard, D.E. Johnson, W.K. Tao, R. Meneghini, L.Liao. "A melting-layer model for passive/active microwave remote sensing applications. Part I: Model formulation and comparison with observations." *Journal of Applied Meteorology*, vol. 40, pp. 1145-1163, 2001.
22. K.B. Katsaros, P.W. Vachon, W.T. Liu, P.G. Black. "Microwave remote sensing of tropical cyclones from space." *Journal of Oceanography*, vol. 58, no. 1. pp.137-151, 2002.
23. S. Sorooshian, X. Gao, K. Hsu, R.A. Maddox, Y. Hong, H.V. Gupta, B. Imam. "Diurnal variability of tropical rainfall retrieved from combined GOES and TRMM satellite information." *Journal of Climate*, vol 15, no. 9. pp. 983-1001, 2002.
24. J.R. McCollum, W.F. Krajewski, R.R. Ferraro, M.B. Ba. "Evaluation of biases of satellite rainfall estimation algorithms over the continental United States." *Journal of Applied Meteorology*, vol. 41, no. 11. pp. 1065-1080. 2002.
25. F.T. Ulaby, M. Razani, C.D. Myron. "Effects of vegetation cover on the microwave radiometric sensitivity to soil moisture." *IEEE Transactions on Geoscience and Remote Sensing*, vol. GE-21, 1983.
26. F.T. Ulaby, R.K. Moore, A.K. Fung, Microwave remote sensing: active and passive, vol. 111-Volume scattering and emission theory, advanced systems and applications. Dedham, MA: Artech House, Mar. 1986.
27. T.J. Schmugge, T.J. Jackson, H.L. Mckim. "Survey of methods for soil moisture determination." *Water Resources Research*, vol. 16, pp. 961-979. 1980.
28. T.J. Jackson, D.M. Le Vine, N.Y. Hsu, A. Oldak, P.J. Starks, C.T. Swift, J.D. Isham, M. Haken. "Soil moisture mapping at regional scales using microwave radiometry: the southern great plains hydrology experiment." *IEEE Transactions on Geoscience and Remote Sensing*, vol. 37. no. 5. pp. 2136-2151. 1999.
29. T. Schmugge, T.J. Jackson, W.P. Kustas, J.R. Wang. 1992. "Passive microwave remote sensing of soil moisture: results from HAPEX, FIFE and MONSOON 90."

- ISPRS Journal of Photogrammetry and Remote Sensing. vol. 47, pp. 127-143. 1992.
30. V. Lakshmi. "Special sensor microwave imager data in field experiments: FIFE-1987." *Int. J. Remote Sensing*, vol. 19, 1998.
 31. F.T. Ulaby, M. Razani, M.C. Dobson. "Effects of vegetation cover on the microwave radiometric sensitivity to soil moisture." *IEEE Transactions on Geoscience and Remote Sensing*, vol. GE-21, 1983.
 32. E.G. Njoku, D. Entekhabi, "Passive microwave remote sensing of soil moisture," *Journal of Hydrology*, vol. 184, pp. 101-129, 1996.
 33. J.W. Wilson, S.H. Yueh, S.J. Dinardo, S.L. Chazanoff, A. Kitiyakara, F.K. Li, Y. Rahmat-Samii. "Passive active L- and S-band (PALS) microwave sensor for ocean salinity and soil moisture measurements". *IEEE Transactions on Geoscience and Remote Sensing*, vol. 39, May 2001.
 34. E.G. Njoku, W. Wilson, S. Yueh, F. Li, S. Dinardo, T. Jackson, V. Lakshmi, and J. Bolten. "Observations of soil moisture using a passive and active low frequency microwave airborne sensor during SGP99". *IEEE Transactions on Geoscience and Remote Sensing*, vol. 40, pp. 2659-2673, 2002.
 35. T.J. Jackson and A. Y. Hsu, "Soil moisture and TRMM Microwave Imager relationships in the Southern Great Plains 1999 (SGP99) Experiment". *IEEE Transactions on Geoscience and Remote Sensing*, vol. 39, pp. 1632-1642, 2001.
 36. D.C. Zehrhuhs, "Temperature and soil moisture studies using in-situ and remotely sensed data in Little Washita, Oklahoma and Little River, Georgia watersheds." Masters Thesis, Department of Geological Sciences, University of South Carolina, 2001.
 37. P.C. Dubois, J. van Zyl, and T. Engman. "Measuring soil moisture with imaging radars." *IEEE Transactions on Geoscience and Remote Sensing*, vol. 33, pp. 915-926, 1995.
 38. Y. Du, F.T. Ulaby, M.C. Dobson. "Sensitivity to soil moisture by active and passive microwave sensors." *IEEE Transactions on Geoscience and Remote Sensing*. vol. 38. 105-114, 2000.
 39. J.P. Wigneron, P. Ferrazzoli, J.C. Calvet, Y. Kerr, and P. Bertuzzi, "A parametric study on passive and active microwave observations over a soybean crop," *IEEE Transactions on Geoscience and Remote Sensing*, vol. 37, pp. 2728-2733, 1999.
 40. T. J. Jackson and T. J. Schmugge, "Vegetation effects on the microwave emission of soils," *Remote Sensing of the Environment*, vol. 36, pp. 203-212, 1991.
 41. J.P. Wigneron, A. Chanzy, J.C. Cavet, N.Bruguir, "A simple algorithm to retrieve soil moisture and vegetation biomass using passive microwave measurements over crop fields." *Remote Sensing of the Environment*. vol. 51, pp. 331-341, 1995.
 42. M.C. Dobson, F.T. Ulaby, M.T. Hallikainen, M.A. El-Rayes, "Microwave dielectric behavior of wet soil-part II: dielectric mixing models" *IEEE Transactions on Geoscience and Remote Sensing*, vol. GE-23, pp. 35-46, 1985.
 43. B.J. Choudhury, 1990. "Monitoring arid lands using AVHRR-observed visible reflectance and SMMR-37 GHz polarization difference." *International Journal of Remote Sensing*, vol. 11, pp. 1949-1956.

44. Chauhan, D. LeVine, and R. Lang, "Use of discrete scatter model to predict active and passive microwave sensor response to corn: comparison of theory and data." IEEE Transactions on Geoscience and Remote Sensing. vol. 32, pp. 416-426, 1994.
45. P.E. O'Neill, N.S.Chauhan, T.J. Jackson. "Use of active and passive microwave remote sensing for soil moisture estimation through corn." International Journal of Remote Sensing, vol. 17, pp. 1851-1865, 1996.
46. N.S. Chauhan. "Soil moisture estimation under a vegetation cover: combined active passive microwave remote sensing approach", International Journal of Remote Sensing, vol. 18, pp. 1079-1097, 1997.

Field Site	Flight Line	Vegetation Cover	Vegetation Water Content (kg m ⁻²)
2	10	Range	0.16
3	10	Range	2.38
4	10	Range	0.48
5	10	Range	0.34
21	9	Wheat (harvested)	0.12
22	9	Wheat (harvested)	0.02
23	9	Wheat (harvested)	0.36
24	12	Bare	0.00
25	12	Corn	7.18
26	12	Corn	5.19
27	12	Alfalfa	1.01

Table I. Field Characteristics within the Little Washita Watershed during SGP99.

R ²	Channels
.904	lh
.908	lh, lv
.92	lh, lv, sh
.92	lh, lv, sh, sv

Table IIa. Passive channels providing the highest correlation with in-situ soil moisture in the 0-0.5 cm range (in all fields) using 1, 2, 3 and 4 channels.

R ²	Channels
.341	svv
.582	lh, svv
.664	lh, lvv, svv
.699	lh, lvv, svv, shhv

Table IIb. Active channels providing the highest correlation with in-situ soil moisture in the 0-0.5 cm range (in all fields) using 1, 2, 3 and 4 channels.

Regressed days (Predicted)	Using Passive Channels	Using Active Channels
	Standard Error (%GSM)	Standard Error (%GSM)
9, 12, 14 (11, 13)	1.39	3.62
9, 11, 13 (12, 14)	2.01	2.56
11, 12, 14 (9, 13)	2.22	3.52
12 13, 14 (9,11)	1.94	5.3
9, 11 (12, 13, 14)	1.83	2.63
11, 14 (9, 12, 13)	1.90	3.39
11, 13 (9, 12, 14)	2.19	3.15

Table III. Standard error (% gravimetric soil moisture) of the statistically predicted soil moisture and the in-situ soil moisture over all vegetation types, using the passive and active PALS channels.

(a) Media & Sensor Parameters	
Vegetation:	
Single scattering albedo, ω	0
Opacity coefficient, b	0.1, 0.19
Soil:	
Roughness coefficients, h (cm) and Q	0.2, 0.2
Bulk density (g cm^{-3})	1.28
Sand and clay mass fractions, s and c	0.3, 0.2
Sensor:	
Viewing angle, θ (deg)	39
Frequency, f (GHz)	1.4, 2.7
Polarization	H, V
(b) Media Variables	
Land Surface:	
Surface soil moisture, m_g (%)	in-situ
Vegetation water content, w_c (kg m^{-2})	in-situ
Surface temperature, T (K)	in-situ

Table IV. Microwave Radiative Transfer Model inputs.

Regressed days (Predicted)	L-band Standard Error (%GSM)	S-band Standard Error (%GSM)
9, 12, 14 (11, 13)	2.89	1.90
9, 11, 13 (12, 14)	2.01	3.04
11, 12, 14 (9, 13)	0.60	2.03
12 13, 14 (9,11)	2.49	2.41
9, 11 (12, 13, 14)	2.23	3.00
11, 14 (9, 12, 13)	2.48	2.87
11, 13 (9, 12, 14)	2.40	3.69

Table V. The passive model (L- and S-band) was run with inputs of surface parameters from the fields within the Little Washita Watershed. Regressions were performed in the forward scheme on either two or three days of data. The table shows the standard error (% gravimetric soil moisture) of the predicted soil moisture. Notice the increase in error when using the S-band.

a) Media & Sensor Parameters	
Vegetation:	
Opacity coefficient, b	0.1
Stalk reflectivity, R_{st}	0.6
Single scattering albedo, ω	0
Soil:	
Roughness coefficient, σ	0.2
Bulk density (g cm^{-3})	1.28
Sand and clay mass fractions, s and c	0.3,0.2
Sensor:	
Viewing angle, θ (deg)	39
Frequency, f (GHz)	1.26
Polarization	HH
(b) Media Variables	
Land Surface:	
Surface soil moisture, m_g (%)	in-situ
Vegetation water content, w_c (kg m^{-2})	in-situ

Table VI. Parameter inputs for the Dobson scattering model.

Regressed days (Predicted)	Standard Error (%GSM-Low Veg) Dobson Model	Standard Error (%GSM-Low Veg) Dubois Model
9, 12, 14 (11, 13)	4.72	5.28
9, 11, 13 (12, 14)	3.13	3.39
11, 12, 14 (9, 13)	1.41	1.84
12, 13, 14 (9,11)	3.90	4.15
9, 11 (12, 13, 14)	3.00	3.35
11, 14 (9, 12, 13)	2.90	3.37
11, 13 (9, 12, 14)	2.95	3.40

Table VII. The active models (L-band) were run with inputs of surface parameters from the low vegetated fields within the Little Washita Watershed. Regressions were performed in the forward scheme on either two or three days of data. The table shows the standard error (% gravimetric soil moisture) of the predicted soil moisture.

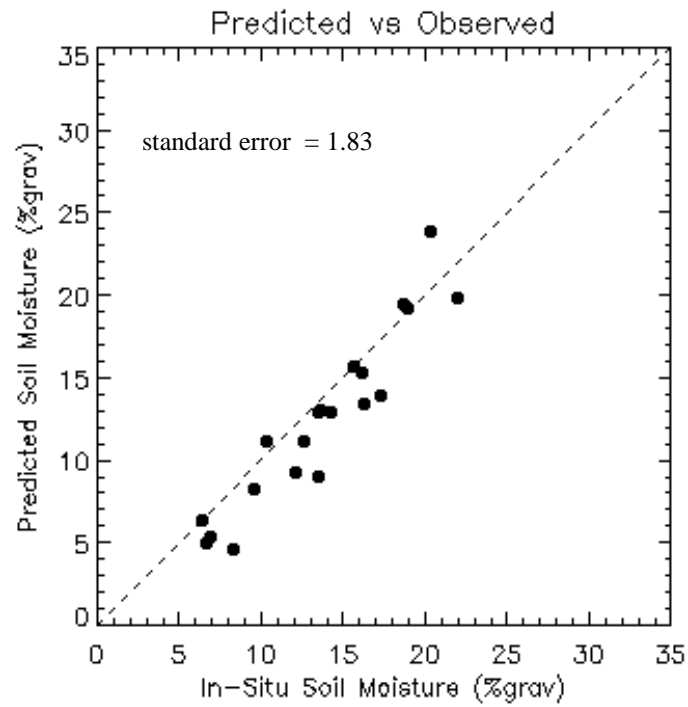


Figure 1. Predicted vs. In-Situ soil moisture using the passive channel statistical regression technique (on days July 9th and 11th) to predict soil moisture for July 12th, 13th and 14th over all fields.

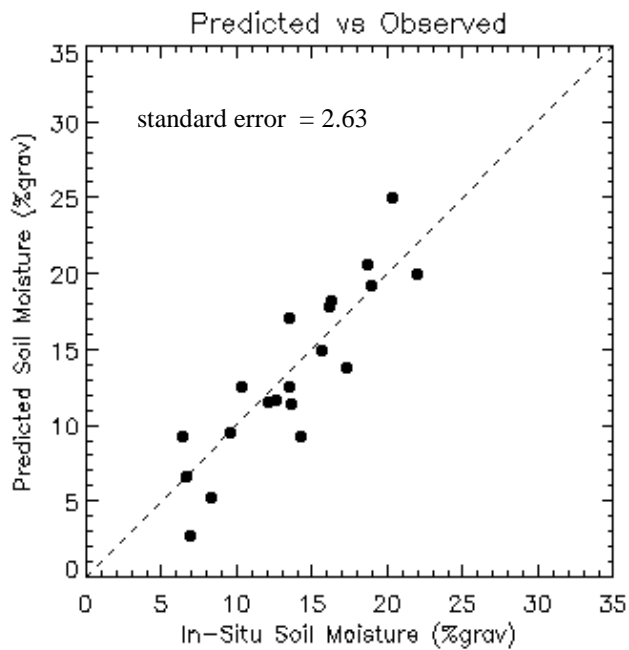


Figure 2. Predicted vs. In-Situ soil moisture using the statistical regression technique (on days July 9th and 11th) to predict soil moisture for July 12th, 13th and 14th over all fields using the active channels.

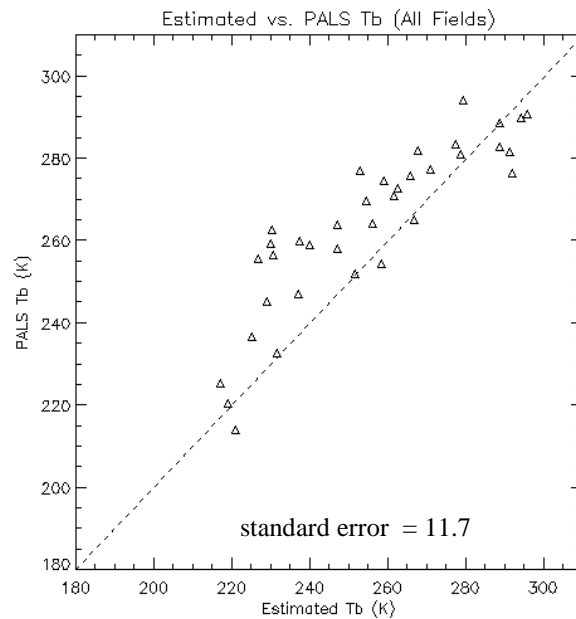


Figure 3. Simulated average brightness temperatures $(\bar{T}_B = T_{BLH} + T_{BLV} / 2)$ computed at frequency 1.4 GHz plotted against observed PALS average brightness temperatures.

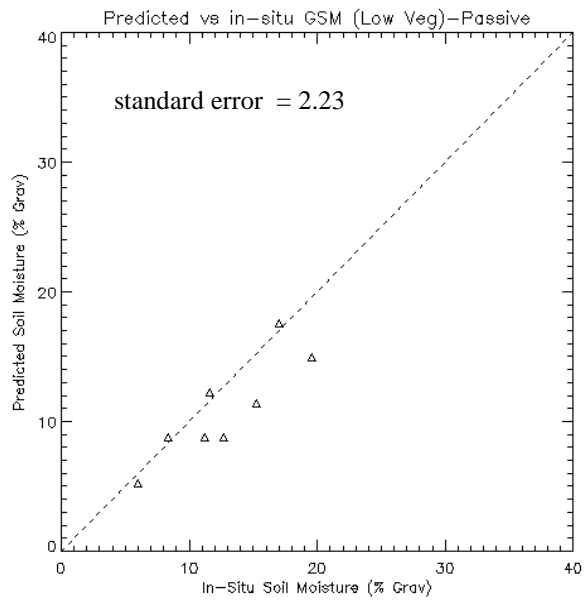


Figure 4. Passive model (L-band) retrieval of soil moisture for low vegetated fields (July 12th, 13th, and 14th).

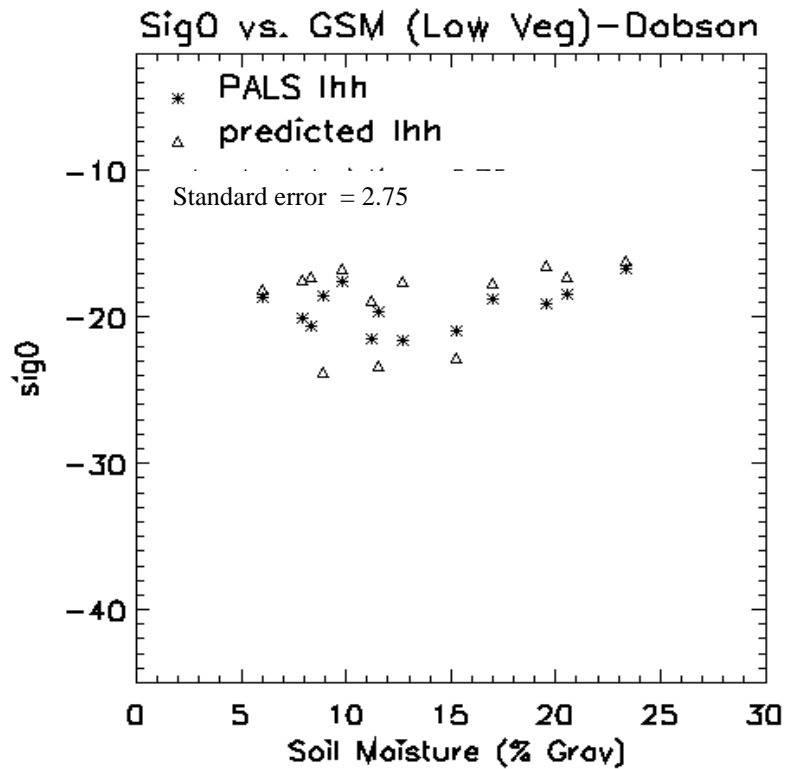


Figure 5. Comparison of modeled σ^0 and PALS σ^0 (LHH) over low vegetated fields with 0 - 5.0cm gravimetric soil moisture using the Dobson model.

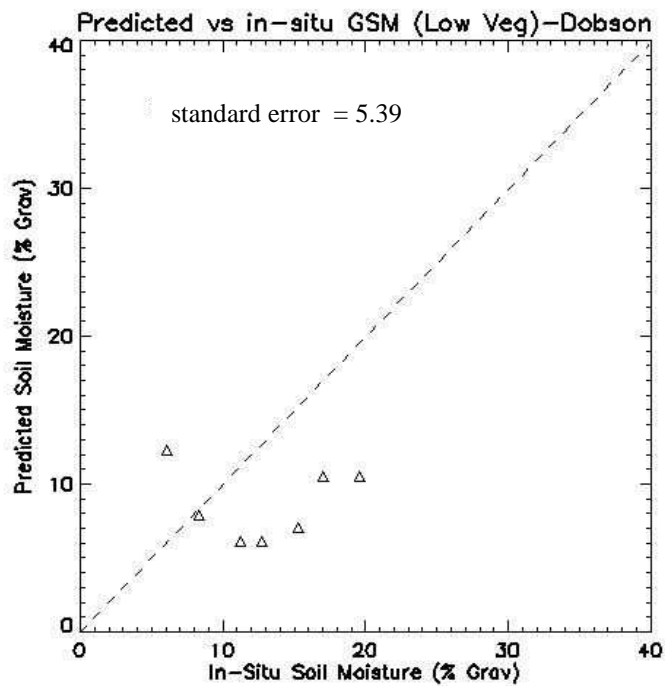


Figure 6. Active model inversion (LHH) (Dobson et al. model) over low vegetated fields. Regression was performed on July 9th, 11th and 13th data, shown is the predicted values for July 12th and 14th.

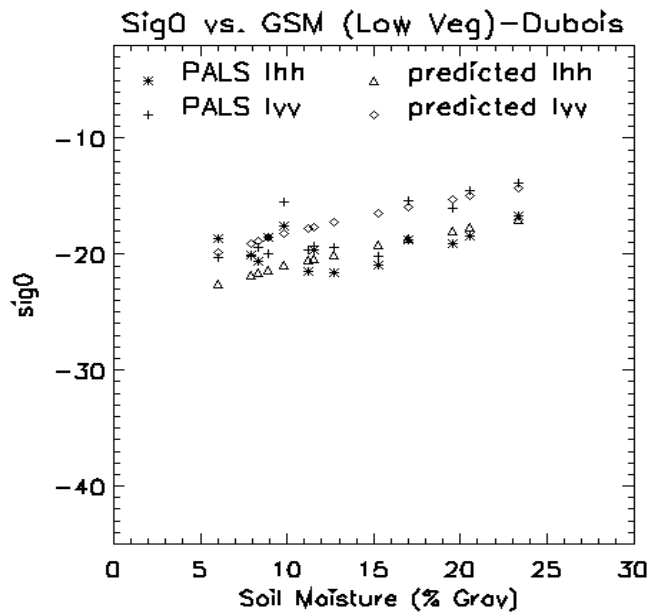


Figure 7. Comparison of modeled σ^0 and PALS σ^0 (LHH, LVV) over low vegetated fields with 0-5.0 cm gravimetric soil moisture using the Dubois model.

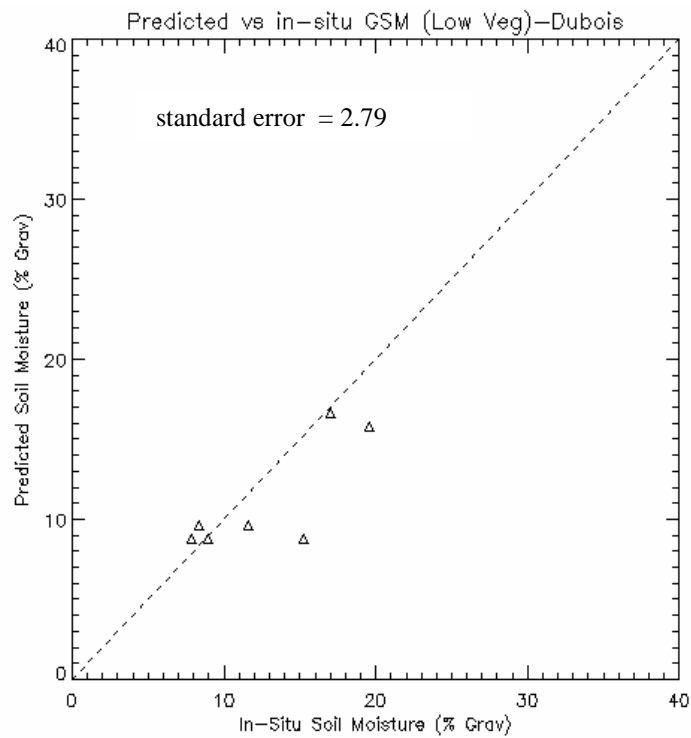


Figure 8. Active model inversion (LHH) (Dubois et al. model) over low vegetated fields. Regressed July 9th, 11th and 13th, predicted for July 12th and 14th.